Published in final edited form as:
Magn Reson Med. 2008 September ; 60(3): 536–541. doi:10.1002/mrm.21699.

Improved Calibration Technique for *in Vivo* Proton MRS Thermometry for Brain Temperature Measurement

M. Zhu[1,2], **A. Bashir**[2], **J. J. Ackerman**[1,2,3], and **D. A. Yablonskiy**[2,4,*]

[1] Department of Chemistry, Washington University, One Brookings Drive, Saint Louis, Missouri 63130, United States

[2] Department of Radiology, Washington University, One Brookings Drive, Saint Louis, Missouri 63130, United States

[3] Department of Internal Medicine, Washington University, One Brookings Drive, Saint Louis, Missouri 63130, United States

[4] Department of Physics, Washington University, One Brookings Drive, Saint Louis, Missouri 63130, United States

Abstract

The most common MR-based approach to non-invasively measure brain temperature relies on the linear relationship between the ^{1}H MR resonance frequency of tissue water and the tissue's temperature. Herein we provide the most accurate *in vivo* assessment existing thus far of such a relationship. It was derived by acquiring *in vivo* MR spectra from a rat brain using a high field (11.74 T) MRI scanner and a single-voxel MR spectroscopy technique based on a LASER pulse sequence. Data were analyzed using three different methods to estimate the ^{1}H resonance frequencies of water and the metabolites NAA, Cho and Cr, which are employed as temperature-independent internal (frequency) references. Standard modeling of frequency-domain data as composed of resonances characterized by Lorentzian line shapes gave the tightest resonance-frequency *vs.* temperature correlation. An analysis of the uncertainty in temperature estimation has shown that the major limiting factor is an error in estimating the metabolite frequency. For example, for a metabolite resonance linewidth of 8Hz, signal sampling rate of 2Hz and SNR of 5, an accuracy of about 0.5°C can be achieved at a magnetic field of 3T. For comparison, in the current study conducted at 11.74 T, the temperature estimation error was about 0.1°C.

INTRODUCTION

Proton (^{1}H) MRS thermometry provides a unique non-invasive method to monitor changes in brain temperature or to quantify absolute brain temperature. The MR frequency of water protons depends on temperature, and it changes with a coefficient of about −0.01 ppm/°C (1). It has been shown by means of magnetic resonance imaging (2) and spectroscopy that this approach can be used for *in vivo* non-invasive temperature mapping (3) and tracking of changes in tissue temperature during functional activation (4). The possibility to quantify absolute brain temperature by monitoring the difference between the water resonance frequency and a temperature independent metabolite resonance frequency (internal reference) has also been demonstrated (5,6).

*Address correspondence and reprint requests to: Dmitriy A. Yablonskiy, Ph.D., Biomedical Magnetic Resonance Laboratory, Campus Box 8227, Mallinckrodt Institute of Radiology, Washington University School of Medicine, 660 South Euclid Avenue, St. Louis, Missouri 63110, USA, YablonskiyD@mir.wustl.edu.

The ^{1}H resonance of the N-acetyl-aspartate (NAA) methyl group is most often used to provide a temperature independent internal reference frequency for *in vivo* temperature quantification in brain tissue due to the relatively high concentration of NAA as compared to other metabolites (5–11). However, because of the small temperature/water-chemical-shift correlation coefficient and low NAA signal amplitude (NAA concentration in the normal brain tissue is about 10,000 times smaller than the water concentration) the accuracy of the method is limited. Two major factors define this accuracy: (i) the predetermined temperature *vs.* ^{1}H MR water frequency correlation (~ − 0.01 ppm/°C) and (ii) the accuracy in estimating the internal reference (metabolite) ^{1}H resonance frequency. Existing literature data suggest there is substantial room for improvement in obtaining a more accurate, internally referenced, calibration curve. This topic is the principal focus of this paper.

MATERIALS AND METHODS

Animal Preparation

Male Sprague-Dawley rats (n = 3) weighing ~300–400 g were initially anesthetized with a ketamine/xylazine combination anesthesia (72.9 mg/kg and 10.4 mg/kg respectively) and given time to stabilize. The animals were then restrained in a prone position within a stereotaxic head-frame (Kopf, Inc., USA) and maintained in an anesthetized state by breathing 1.2% isoflurane in 100% O_2 through a nosepiece. The subjects' heads were shaved, a midline incision performed, and, after carefully removing a small area of scalp and membrane layers around Lambda area, the skull was exposed. A 1-mm diameter burr hole was drilled through the skull 2 – 3 mm anterior to and lateral from the Lambda. In an attempt to prevent any MR measurement error from field inhomogeneities created by the surgical procedure, the burr hole was purposefully placed 3 – 4 mm posterior from the projected MRS voxel site near the region of the Bregma. A small amount of petroleum jelly (Vaseline) was applied at the burr-hole site to prevent bleeding.

Individual subjects were then transferred to a laboratory-constructed Teflon head holder and the head restrained with ear and tooth bars. A single-turn, 1.0-cm diameter transmit-receive (transceiver) surface coil was placed on the shaved head directly over the brain. A 1-mm diameter fiber-optic temperature probe (Model Luxtron 755; Luxtron Corp., USA) was inserted at a 45° angle into right side of the brain through the burr-hole to a vertical depth of ~5 mm (Fig. 1). Each subject's head was carefully insulated with cotton batting to diminish internal temperature gradients that would degrade the calibration. Another fiber-optic probe was inserted 7 cm deep into the animal's rectum to monitor body temperature. Temperature probes were calibrated before and after each experiment to be within an accuracy of ± 0.05 °C. The animal's torso was put on a circulating water pad (Model D10-B3; Thermo Haake, Karlsruhe, Germany) to maintain the body temperature ~ 37.5 °C. The same water circulation system was also used to vary body/brain temperature for calibration measurements. Anesthesia was maintained with 1.2% isoflurane (in 100% O_2) throughout the entire MR experiment.

During the calibration experiment, each subject's body was slowly and continuously cooled from 37.5 °C to ~30 °C by controlling the temperature of water circulating under the torso (abdomen) over about 2.5-hour period. In practice, a small amount of ice was mixed with the water in circulator's reservoir. Body temperature dropped slightly faster than brain temperature. The initial body/brain temperature difference was + 0.1 °C at the fiber-optic probe site (body warmer than brain); at the end of the cooling period, the differential changed to ~ − 0.1 °C ((body cooler than brain). This slow cooling rate (~7 °C temperature drop in 2.5 hours) was designed to assure adequate heat exchange and temperature equilibration within the brain.

Concomitantly with progressive cooling of each subject, single voxel ^{1}H MR spectroscopy data was acquired with parameters as described below. The fiber-optic probes continuously recorded brain and body (core) temperature during the course of the experiment.

NMR Experiments

All experiments were performed with an MR scanner based on a Magnex (Yarnton, UK) 11.74-T (500-MHz) 26-cm clear-horizontal-bore magnet with an 8-cm inner-diameter gradient and shim assembly (maximum gradient strength 120 gauss/cm, rise time 200 μs). The system was controlled by a Varian (Palo Alto, CA) INOVA console. The single voxel localization by adiabatic selective refocusing (LASER) pulse sequence (12) was employed for spectroscopy experiments during the cooling process. The LASER voxel was placed in a location closely approximating that of the tip of the temperature probe but on the contralateral side of the brain (see Fig. 1). Data acquisition was performed every 0.5 hr with the following acquisition parameters: 4 kHz bandwidth, 2048 data points, TR = 1.6 s, TE = 75 ms, 512 ms acquisition time, $3 \times 3 \times 3$ mm^3 voxel size, 200 free induction decays (FIDs). No water suppression was applied. Shimming was re-optimized prior to each acquisition of 200 FIDs (i.e., every 0.5 hr).

Each individual FID was stored separately and phase corrected. Each set of 200 FIDs, collected at 0.5-hr time increments, was divided into two summed (averaged) sets of FIDs: the first 100 FIDs collected making up one summed data set and the second 100 FIDs collected making up the second summed data set. Considering each set of 200 FIDs as a pair of sequential 100 FID data sets minimized the influence of temperature drift during data acquisition. In one subject, a total of four pairs of 100 FID data sets were obtained; for each of the other two subjects, five pairs of 100 FID data sets were obtained. The final temperature calibration employed data from all three animals: 14 pairs of 100 FID data sets.

Resonance Frequency Analysis

Metabolite and water ^{1}H resonance frequencies were estimated by three different methods. The first method employed a frequency domain analysis using MestReC software (Mestrelab Research, Spain). An exponential apodizing function resulting in a 3-Hz line broadening was applied to the FID's before Fourier transformation. A zero order phase correction was then manually applied before the water and NAA resonance frequencies were estimate by the "peak picking" algorithm in MestReC.

The second approach employed a time domain analysis using jMRUI software (13) (URL http://www.mrui.uab.es/mrui/) in two steps. First, the water signal was modeled as a mono-exponentially decaying sinusoid (a single component) using the Hankel Lanczos Total Least Squares (HLTLS) algorithm (14) and its resonance frequency estimated. Second, the water signal was removed (filtered) from the FID by Hankel Lanczos Singular Value Decomposition (HLSVD) algorithm (15) in a 2 ppm range around the water resonance frequency. The residual signal was then used to estimate the NAA resonance frequency using the HLTLS algorithm.

The third approach employed a standard frequency domain line shape analysis using MATLAB software. The FID was zero filled to a total of 4096 complex data points, Fourier transformed, and zero order phase corrected. The water and NAA resonances (100 Hz around each) were separately modeled as Lorentzian line shapes and the frequencies estimated.

RESULTS

An example of a single voxel frequency domain ^{1}H spectrum from *in vivo* rat brain is shown in Fig. 2 without line broadening. The water and metabolite resonances are well resolved. The typical linewidth for the NAA ^{1}H resonance in our study is 5–10 Hz and the typical SNR is about 5–7.

Figure 3 shows the temperature calibration results (using NAA as an internal frequency reference) from the three approaches to estimating frequencies: Fig. 3A shows the results from MestReC modeling, Fig. 3B shows the results from jMRUI time domain modeling, and Fig. 3C shows the results from Lorentzian line shape modeling in the frequency domain. The temperature *vs.* resonance frequency data pairs were modeled using the following linear equation:

$$T_b = 36 + \alpha \cdot (F_w - F_{ref} - F_0). \quad [1]$$

Here T_b is the brain tissue temperature in degrees Centigrade measured by the optical probe, F_w and F_{ref} are water and internal reference (NAA) ^{1}H resonance frequencies in ppm, and α is the temperature *vs.* frequency correlation coefficient (slope). This equation is written in such a form that F_0 is the frequency difference between water and NAA resonances at 36 °C. Both F_0 and α are fitting parameters. The results from all three correlations in Fig. 3 are as follows:

$$A{:}\alpha = -105.82 \pm 2.93^{\circ}C/ppm, \quad F_0 = -2.6745 \pm 0.0006\, ppm; \quad R^2 = 0.98 \quad [2]$$

$$B{:}\alpha = -106.87 \pm 3.46^{\circ}C/ppm, \quad F_0 = -2.6745 \pm 0.0007\, ppm; \quad R^2 = 0.97 \quad [3]$$

$$C{:}\alpha = -103.80 \pm 1.90^{\circ}C/ppm, \quad F_0 = -2.6759 \pm 0.0004\, ppm; \quad R^2 = 0.99 \quad [4]$$

From the 95% prediction limits in the graphs, it can be seen that Lorentzian line shape modeling in frequency domain (Fig. 3C) gave the best brain temperature *vs.* water-NAA chemical shift difference correlation.

Further analysis of the data using Creatine (Cr) and Choline (Cho) ^{1}H resonances as internal frequency references also demonstrated strong correlation between brain temperature and water-Cr (or water-Cho) frequency difference. These resonances were analyzed using Lorentzian frequency domain line shape modeling only since it gave the most accurate correlation curve with NAA as the reference resonance. Results are shown in Fig. 4. Linear correlation analysis with Eq. [1] produced the following results:

$$Cr{:}\alpha = -101.70 \pm 1.72^{\circ}C/ppm, \quad F_0 = -1.6585 \pm 0.0004\, ppm; \quad R^2 = 0.99 \quad [5]$$

$$Cho{:}\alpha = -106.08 \pm 2.07^{\circ}C/ppm, \quad F_0 = -1.4755 \pm 0.0004\, ppm; \quad R^2 = 0.98 \quad [6]$$

DISCUSSION

To our knowledge, this is the first report of *in vivo* MRS brain temperature *vs.* ^{1}H resonance frequency calibration that has been performed at ultra high field in rat. Comparisons of this study and previously reported *in vivo* MRS brain temperature calibration studies are summarized in table 1. The correlation coefficient α reported herein has a larger absolute value than those reported previously, irrespective of which metabolite (NAA, Cr or Cho) is used for internal reference. These results also demonstrate the best linear regression fitting quality (largest R^2).

Equation [1] allows the uncertainty in measuring brain temperature by means of water/metabolite frequency difference, δT_b, to be estimated. If we assume that the parameter α does not change with the brain tissue content/composition and physiological status of the brain (see discussion below), the following simple equation can be derived:

$$\delta T_b \approx \delta\alpha \cdot |F_w - F_{ref} - F_0| + |\alpha| \cdot \delta F_0 + |\alpha| \cdot (\delta F_w + \delta F_{ref}). \quad [7]$$

The first term defines error due to uncertainty in estimating parameter α. Since in the physiological range the frequency difference is about 0.01 ppm, and δα in our derived equations is about 2°C/ppm, this term leads to a rather small uncertainty of about 0.02 °C. The second term in Eq. [7] defines an error due to uncertainty in estimating parameter F_0. Since $|\alpha| \approx 100$ and $\delta F_0 = 0.0004$ ppm, this error is also rather small, about 0.04 °C. Hence, the major error in this estimate comes from the third term, which depends upon the uncertainties in estimating the ^{1}H frequencies of water and metabolite signals. A similar conclusion has been reached by Childs *et al* (7) based on numerical simulations. The limiting part here is, of course, the modeling of the metabolite ^{1}H resonance, which has an amplitude four orders of magnitude less than the water resonance. Hence, to achieve a 1°C temperature estimation accuracy requires an accuracy in metabolite frequency estimation of 0.01 ppm. The metabolite ^{1}H resonance frequency measurement error δF_{ref} can be estimated by making use of the theoretical expression (16):

$$\delta F_M = \frac{\pi \cdot \Delta F_{ref}}{SNR_{ref} \cdot \nu_0} \cdot \sqrt{\pi \cdot \Delta F_{ref} \cdot \Delta t}, \quad [8]$$

where ΔF_{ref} is the linewidth of metabolite signal in Hz, Δt is signal sampling dwell time in sec, ν_0 is the scanner frequency in MHz, and SNR is the signal-to-noise ratio. For example, for $\Delta F_{ref} = 10Hz$, $\nu_0 = 64Mhz$ (1.5 T scanner), $\Delta t = 0.001$ sec, and metabolite SNR of 10, the accuracy of temperature estimation is about 1 °C. For comparison, in the current study the frequency estimation error δF_{ref} based on Eq. [8] is ~ 0.0008 ppm, which translates to a temperature estimation error of ~ 0.1 °C.

Several other issues should be taken into consideration when estimating MR-based temperature measurement error. First, the MR signal is never purely Lorentzian. This is because macroscopic magnetic field inhomogeneities contribute to signal decay, hence highly accurate resonance frequency estimation strongly depends on meticulous field homogeneity shimming. However, complete elimination of field inhomogeneities is not possible in real human and animal experiments. It was previously demonstrated that incorporating information regarding field inhomogeneities in spectroscopy data processing leads to a more robust modeling of the FID signal (17,18) and, hence, could lead to more accurate temperature estimates.

A second, more vexing issue, is that the tissue water resonance in brain contains multiple components. In addition to the main resonance, there exists a contribution from a component with long T2 relaxation time constant (presumably extracellular fluid) with volume fraction of about 10% and shifted by about 0.04 ppm (19). There might also be small contributions from other components with short T2 (20,21) and blood (19), however their influence is expected to be very small, especially for spectroscopic sequences with echo times longer than T2 of these "short-lived" components. A similar "multi-component problem" exists for metabolite signals. Although signals from NAA, Cho and Cr are each modeled as a single ^{1}H resonance in this study, the spectral regions in which these metabolite resonances occur in the brain all contain signals from more than one metabolite specie, and the ^{1}H resonances from these different species, in most cases, occur at different frequencies. For example, the "NAA" methyl group resonance, which is located around 2.0 ppm, is actually composed of resonances from N-acetyl aspartate (NAA) and N-acetylaspartylglutamate (NAAG). Due to the structural similarity of the two compounds, their resonances are separated by only 0.03 ppm (22). The "Cr" resonance observed around 3.0 ppm in this study refers to resonances from both creatine (Cr) and phosphocreatine (PCr). The singlet resonances from methyl protons of both compounds differed by only 0.002 ppm (23). Similarly, the "Cho" resonance observed at 3.2 ppm actually includes contributions from free choline (Cho), glycerophosphorylcholine (GPC) and phosphorylcholine (PC). The resonance frequency of the trimethylamine group from free choline is separated from GPC and PC by about 0.02 ppm (23). Distinguishing the individual resonances that characterize each of these components is currently not possible with *in vivo* brain MR spectroscopy. Thus, the magnitude of the effect of the multi-component structure of water and metabolite signals on *absolute* temperature determination is not clear but could be significant if component concentrations vary across the brain or under challenge of neurological disorder. Indeed, the presence of a putative component concentration gradient (or inhomogeneity profile) across the brain would generate a corresponding apparent resonance frequency gradient for water and the chosen internal reference specie. This would degrade the accuracy of individual temperature determinations. Nevertheless, even in this situation, the derived relationships, Eqs. [1] – [6], would still determine accurate *changes* in local brain temperature under different *transient* conditions (brain cooling for example) because it is very unlikely that local brain tissue component content would also change transiently.

Another important issue that can influence the accuracy of temperature determination is the potential dependence of the water resonance signal frequency on tissue chemical environment, such as concentration of macromolecules, proteins and different ions. While *in vivo* studies of these phenomena are yet to be conducted, *in vitro* studies have demonstrated that within the physiological setting the frequency vs. temperature coefficient remains practically independent of the protein concentration (6), tissue type (24), and pH (5,25,26).

In addition to exploring endogenous markers like NAA, Cho and Cr, the use of exogenous temperature sensitive probe molecules to monitor temperature change in biological systems has been explored during the past decade. Typically employed are paramagnetic lanthanide complexes with temperature sensitive components (27–32). Specific ^{1}H sites in these molecules have resonance frequencies tens or hundreds times more temperature sensitive than water. One such example is (TmDOTMA^{-}). The ^{1}H temperature coefficient of the methyl group in this molecule is reported to be 0.57 ppm/°C, almost 60 times greater than observed with water. Given this large temperature sensitivity, excellent results using this probe molecule have been reported with phantom/test samples [*e.g.*, 0.1–0.2 °C accuracy has been reported (29)]. Despite certain advantages, the technique presents several serious challenges for *in vivo* studies. First, because these agents are exogenous, they must be introduced to the body. Like the commonly used MRI contrast agents, the temperature sensitive lanthanide complexes do not cross the blood-brain barrier (BBB) (29). Thus, issues

regarding routes of administration, tissue distribution, and toxicity require solutions. Further, these complexes are efficiently cleared out of the body by the kidneys. Thus, the initially low concentration of the agent is reduced further by excretion, limiting the time frame for imaging. Nevertheless, the concept of exogenous temperature sensitive probes for *in vivo* applications is quite new and various probe molecules are still under development. Because the temperature sensitivity of exogenous probes is among the best of the various MR thermometry approaches, their development remains an area of considerable research activity.

In conclusion, this work improves the accuracy of phenomenological equations relating brain temperature to the ^{1}H resonance frequencies of water and metabolites. A theoretical analysis of expected errors in temperature evaluation is also developed. Findings presented herein allow a temperature evaluation accuracy of ~ 0.1 °C to be achieved at high field.

Acknowledgments

This study was supported by NIH Grants RO1-NS41519 and R24-CA83060 (Small Animal Imaging Resource Program)

References

1. Hindman JC. Proton resonance shift of water in the gas and liquid states. Journal of Chemical Physics. 1966; 44(12):4582–4592.
2. Parker DL, Smith V, Sheldon P, Crooks LE, Fussell L. Temperature distribution measurements in two-dimensional NMR imaging. Med Phys. 1983; 10(3):321–325. [PubMed: 6877179]
3. Kuroda K, Suzuki Y, Ishihara Y, Okamoto K, Suzuki Y. Temperature mapping using water proton chemical shift obtained with 3D-MRSI: feasibility in vivo. Magn Reson Med. 1996; 35(1):20–29. [PubMed: 8771019]
4. Yablonskiy DA, Ackerman JJ, Raichle ME. Coupling between changes in human brain temperature and oxidative metabolism during prolonged visual stimulation. Proc Natl Acad Sci U S A. 2000; 97(13):7603–7608. [PubMed: 10861022]
5. Cady EB, D'Souza PC, Penrice J, Lorek A. The estimation of local brain temperature by in vivo 1H magnetic resonance spectroscopy. Magn Reson Med. 1995; 33(6):862–867. [PubMed: 7651127]
6. Corbett RJ, Laptook AR, Tollefsbol G, Kim B. Validation of a noninvasive method to measure brain temperature in vivo using 1H NMR spectroscopy. J Neurochem. 1995; 64(3):1224–1230. [PubMed: 7861155]
7. Childs C, Hiltunen Y, Vidyasagar R, Kauppinen RA. Determination of regional brain temperature using proton magnetic resonance spectroscopy to assess brain-body temperature differences in healthy human subjects. Magn Reson Med. 2007; 57(1):59–66. [PubMed: 17139620]
8. Katz-Brull R, Alsop DC, Marquis RP, Lenkinski RE. Limits on activation-induced temperature and metabolic changes in the human primary visual cortex. Magn Reson Med. 2006; 56(2):348–355. [PubMed: 16791859]
9. Zhu, M.; Ackerman, JJ.; Yablonskiy, DA. MR Spectroscopic Measurement of Inhomogeneous Temperature Distribution in the Rat Brain. Miami: 2005.
10. Kuroda K. Non-invasive MR thermography using the water proton chemical shift. Int J Hyperthermia. 2005; 21(6):547–560. [PubMed: 16147439]
11. Kauppinen RA, Vidyasagar R, Childs C, Balanos GM, Hiltunen Y. Assessment of human brain temperature by (1)H MRS during visual stimulation and hypercapnia. NMR Biomed. 2007 article in press.
12. Garwood M, DelaBarre L. The return of the frequency sweep: designing adiabatic pulses for contemporary NMR. J Magn Reson. 2001; 153(2):155–177. [PubMed: 11740891]
13. Naressi A, Couturier C, Devos JM, Janssen M, Mangeat C, de Beer R, Graveron-Demilly D. Java-based graphical user interface for the MRUI quantitation package. Magma. 2001; 12(2–3):141–152. [PubMed: 11390270]

14. Vanhuffel S, Chen H, Decanniere C, Vanhecke P. Algorithm for Time-Domain NMR Data Fitting Based on Total Least Squares. J Magn Reson. 1994; 110(2):228–237.
15. Pijnappel WWF, van den Boogaart A, de Beer R, van Ormondt D. SVD-based quantification of magnetic resonance signals. J Magn Reson. 1992; 97(1):122.
16. Bretthorst, GL. Bayesian Spectrum Analysis and Parameters Estimation. Berger, J.; Feinberg, S.; Gani, J., editors. New York: Springer-Verlag; 1988. p. 210
17. Webb P, Spielman D, Macovski A. Inhomogeneity correction for in vivo spectroscopy by high-resolution water referencing. Magn Reson Med. 1992; 23(1):1–11. [PubMed: 1734171]
18. Bashir A, Yablonskiy DA. Natural linewidth chemical shift imaging (NL-CSI). Magn Reson Med. 2006; 56(1):7–18. [PubMed: 16721752]
19. He, X.; Yablonskiy, DA. Quantitative BOLD: Separation of Effects from Blood Volume and Oxygen Extraction Fraction. Seattle: 2006.
20. Ernst T, Kreis R, Ross BD. Absolute quantitation of water and metabolites in the human brain. I. Compartments and water. Journal of Magnetic Resonance, Series B. 1993; 102(1):1–8.
21. Whittall KP, MacKay AL, Graeb DA, Nugent RA, Li DK, Paty DW. In vivo measurement of T2 distributions and water contents in normal human brain. Magn Reson Med. 1997; 37(1):34–43. [PubMed: 8978630]
22. Edden RA, Pomper MG, Barker PB. In vivo differentiation of N-acetyl aspartyl glutamate from N-acetyl aspartate at 3 Tesla. Magn Reson Med. 2007; 57(6):977–982. [PubMed: 17534922]
23. Govindaraju V, Young K, Maudsley AA. Proton NMR chemical shifts and coupling constants for brain metabolites. NMR Biomed. 2000; 13(3):129–153. [PubMed: 10861994]
24. Peters RD, Hinks RS, Henkelman RM. Ex vivo tissue-type independence in proton-resonance frequency shift MR thermometry. Magn Reson Med. 1998; 40(3):454–459. [PubMed: 9727949]
25. Lutz NW, Kuesel AC, Hull WE. A 1H-NMR method for determining temperature in cell culture perfusion systems. Magn Reson Med. 1993; 29(1):113–118. [PubMed: 8419730]
26. Martin M, Labouesse J, Canioni P, Merle M. N-acetyl-L-aspartate and acetate 1H NMR signal overlapping under mild acidic pH conditions. Magn Reson Med. 1993; 29(5):692–694. [PubMed: 8505907]
27. Hekmatyar SK, Hopewell P, Pakin SK, Babsky A, Bansal N. Noninvasive MR thermometry using paramagnetic lanthanide complexes of 1,4,7,10-tetraazacyclodoecane-alpha,alpha′, alpha″, alpha ‴-tetramethyl-1, 4,7,10-tetraacetic acid (DOTMA4-). Magn Reson Med. 2005; 53(2):294–303. [PubMed: 15678553]
28. Hekmatyar SK, Poptani H, Babsky A, Leeper DB, Bansal N. Non-invasive magnetic resonance thermometry using thulium-1,4,7,10-tetraazacyclododecane-1,4,7,10-tetraacetate (TmDOTA(-)). Int J Hyperthermia. 2002; 18(3):165–179. [PubMed: 12028635]
29. Pakin SK, Hekmatyar SK, Hopewell P, Babsky A, Bansal N. Non-invasive temperature imaging with thulium 1,4,7,10-tetraazacyclododecane-1,4,7,10-tetramethyl-1,4,7,10-tetraacetic acid (TmDOTMA-). NMR Biomed. 2006; 19(1):116–124. [PubMed: 16404728]
30. Zuo CS, Bowers JL, Metz KR, Nosaka T, Sherry AD, Clouse ME. TmDOTP5-: a substance for NMR temperature measurements in vivo. Magn Reson Med. 1996; 36(6):955–959. [PubMed: 8946362]
31. Zuo CS, Mahmood A, Sherry AD. TmDOTA-: a sensitive probe for MR thermometry in vivo. J Magn Reson. 2001; 151(1):101–106. [PubMed: 11444943]
32. Zuo CS, Metz KR, Sun Y, Sherry AD. NMR temperature measurements using a paramagnetic lanthanide complex. J Magn Reson. 1998; 133(1):53–60. [PubMed: 9654468]

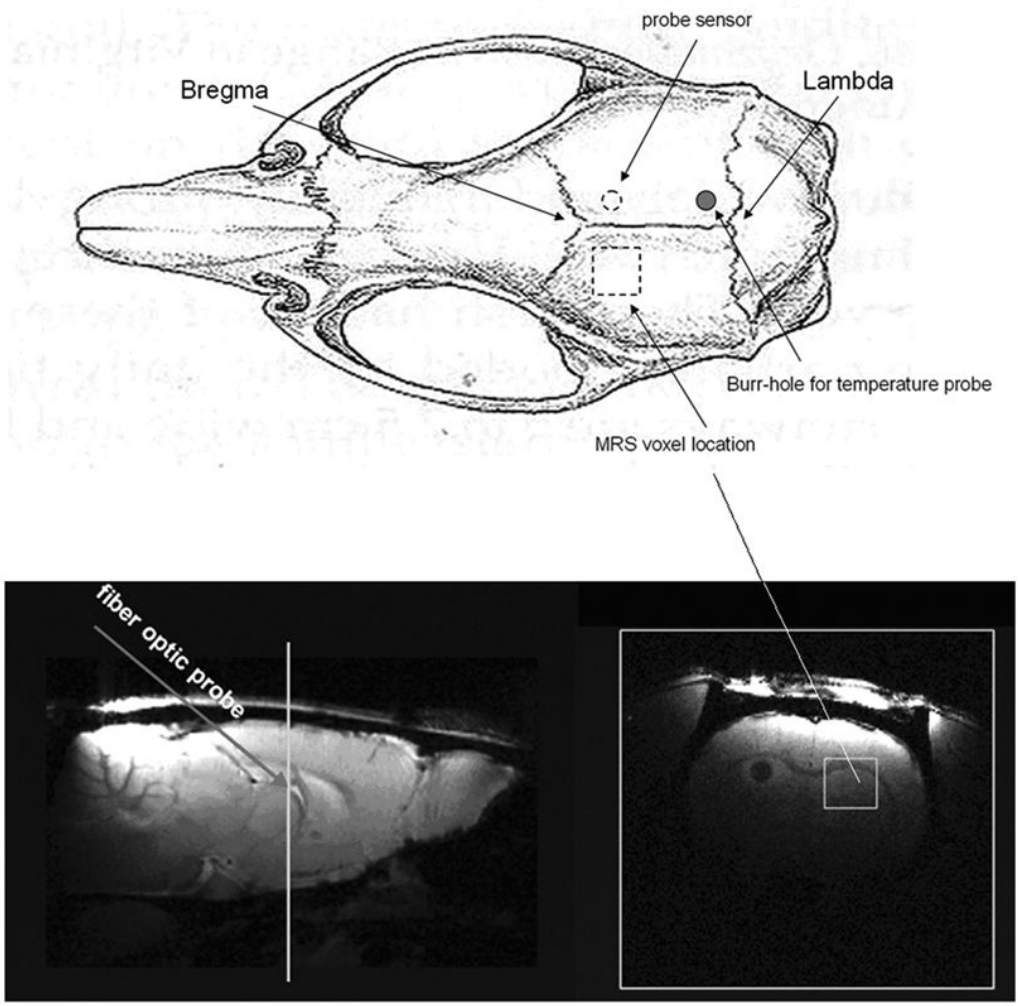

Figure 1.

Temperature probe sensor, burr hole and MRS voxel locations. The upper image is a diagram of rat skull (dorsal view) with the indicated skull land marks: Lambda and Bregma (Paxinos and Watson, *The Rat Brain in Stereotaxic Coordinates*. Second Edition. New York: Academic Press, 1986). The bottom panels are sagital (left) and transaxial (right) images from a rat brain (note the transaxial image is from the plane crossing the white line indicated in the sagital image). The temperature probe was inserted from burr-hole through the skull at a 45° angle and the probe sensor reached the region that neighbored the MRS voxel (dashed circle in the upper sketch, and dark region in the bottom right transaxial brain MR image). The voxel size is $3 \times 3 \times 3$ mm^3 and positioned as indicated.

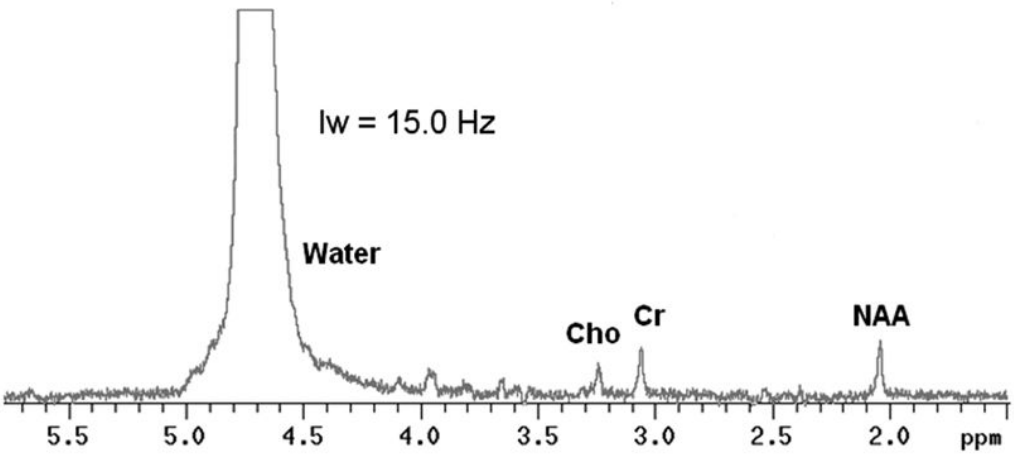

Figure 2.
Example of a single voxel ^{1}H spectrum from *in vivo* rat brain at 11.74 T. Only zero order phase correction was applied to the spectrum. No line broadening filtering was used in this example.

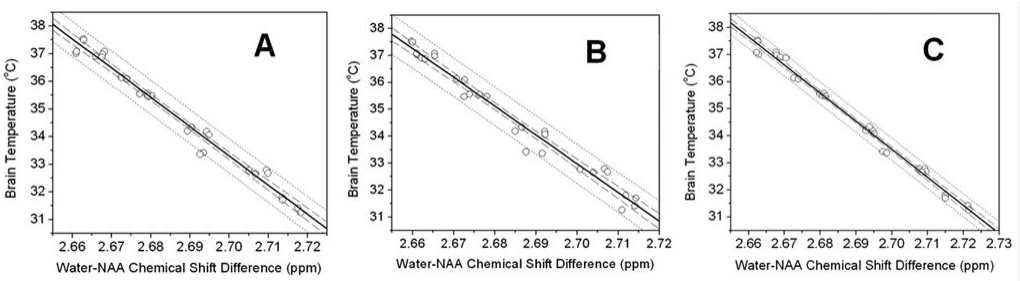

Figure 3.

Correlations between water-NAA ^{1}H resonance frequency and directly measured brain temperature - comparison among three different approaches: A, MestReC modeling; B, jMRUI time domain modleing; C, Lorentzian line shape frequency domain modeling. In each graph, the solid line across the data is the linear least squares fit to the data, the dotted lines provide the 95% prediction limits and the dashed lines represent 95% confidence limit for the linear fitting. See Table 1 and Eqs. [2] – [4] for linear fitting results.

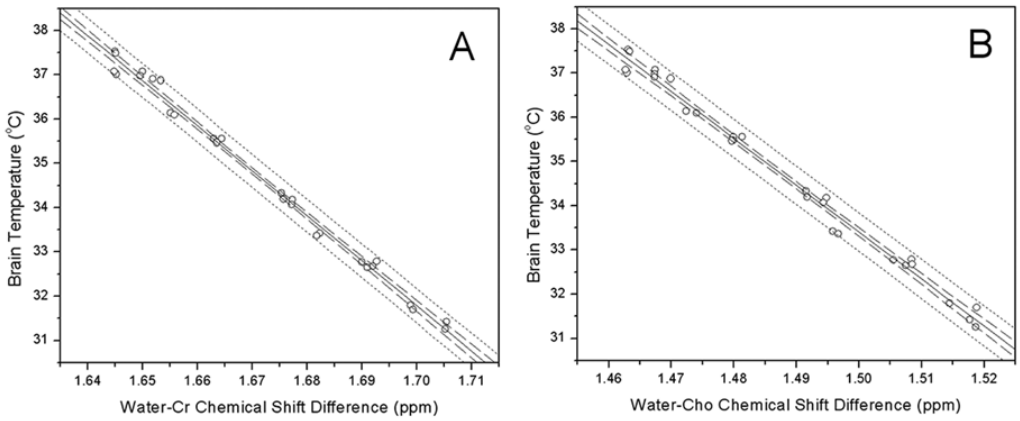

Figure 4.

Correlations between water ^{1}H resonance frequency differences and directly measured brain temperature using A: Creatine (Cr) and B: Choline (Cho) as internal frequency references. Solid lines are the linear least squares fit to the data; dotted lines are 95% prediction limit and dashed lines are 95% confidence limit for the linear fitting 17.

Table 1

Comparison of MRS brain temperature calibration results (temperature *vs.* frequency shift coefficient α in Eq. (1)) measured *in vivo*.

Source	Metabolite	Correlation Coefficient	R^2	Species
Current study	NAA	$\alpha = -103.8 \pm 1.9$	0.99	Rat
	Cr	$\alpha = -101.7 \pm 1.7$	0.99	Rat
	Cho	$\alpha = -106.1 \pm 2.1$	0.98	Rat
Corbett *et al.*, 1999	NAA	$\alpha = -82.33 \pm 6.58$	0.71	Dog
	TMA	$\alpha = -70.11 \pm 6.06$	0.69	
Corbett *et al.*, 1997	NAA	$\alpha = -72.2 \pm 5.0$	0.87	Swine
	TMA	$\alpha = -77.8 \pm 5.5$	0.87	
Cady *et al.*, 1995	NAA	$\alpha = -94.0 \pm 3.7$	N/A	Piglet

Note: In the correlation equation Eq. (1), α represents temperature shift (in degrees Centigrade) *vs.* frequency difference (in ppm) between water and the specific metabolite reference. Other notations: Cr - creatine; Cho - choline; TMA - trimethylamines (equivalent to choline containing compounds in other literatures).